

A Distributed ADMM Approach to Informative Trajectory Planning for Multi-Target Tracking

Soon-Seo Park, Jung-Su Ha, Doo-Hyun Cho and Han-Lim Choi

Abstract—This paper presents a distributed optimization method for informative trajectory planning in multi-target tracking problems. The purpose of such problems is to optimize a sequence of waypoints/control inputs of mobile sensors over a certain future time step to minimize the uncertainty of targets. The planning problem is reformulated as a distributed optimization problem that can be expressed in the form of a subproblem for each target. The subproblems are coupled using the distributed Alternating Direction Method of Multipliers (ADMM). This coupling not only enables the results of each subproblem to be reflected in the optimization process of the other subproblems, but also guides the results of the subproblems to converge to the same solution. In contrast to existing approaches performing trajectory optimization after assigning tasks, the proposed algorithm does not require the design of a heuristic cost function for task assignment, and it can handle both non-myopic trajectory planning and task assignment in multiple target tracking problems simultaneously. In order to reduce the computation time of the algorithm, an edge-cutting method suitable for multiple target tracking problems is proposed, as a receding-horizon control scheme for real-time implementation, which considers the computation time. Numerical examples are presented to demonstrate the applicability of the algorithm.

I. INTRODUCTION

Technological advances in sensor networks allow us to use such systems for monitoring environmental systems such as pollution/atmospheric phenomena, as well as for reconnaissance and surveillance missions in both defense and civilian areas. The capability of sensor networks would also be invaluable for several other applications, including traffic monitoring, forest fire localization, and wildlife tracking [1], [2]. To take full advantage of networked systems, it is crucial to efficiently operate sensing agents to maximize information about the target systems of interest. This problem requires an estimation of the variables of interest through measurements acquired by a sensor while considering the constraints of the system; that is also described as a sensor planning problem that determines the future utilization of sensing agents given the current state of the resources and the environment.

Target tracking is a common application in which the information of interest (i.e., the kinematic state) is inferred largely from sensor measurements that are in proximity to the target. The key challenge in the target tracking problem is to estimate a distribution over the set of possible states based on noisy sensor measurements, instead of directly measuring the states of the target. This kind of problem is generally described as involving partially observable Markov decision processes (POMDPs). The most common approach to deal

with POMDPs is Bayesian filtering that represents the uncertainty of a target's state as a covariance matrix. This measure of uncertainty is combined with various matrices such as the Fisher information (FIM) [3]–[5], mutual information [6], [7], or trace [8], [9], and is then used to optimize the variables that determine the operation of the sensing agents. In the target tracking problem, sensor planning problems are divided into two major classes: (a) Sensor scheduling [10]–[16] and (b) the trajectory planning of mobile sensors [3]–[6], [8], [9], [17]–[21]. Sensor scheduling attempts to select some of the multiple available static sensors at each time step to minimize the weighted sum of all estimation errors over a certain time horizon. A set of constraints on the number of sensors available and/or on energy/communication budgets of the sensor network can be involved in the decision variables. The problem is generally solved by dynamic programming [12]–[15], where all possible schedules are enumerated. The complexity of such an enumeration approach grows exponentially as the horizon increases. To overcome this problem, research has focused on addressing computational challenges, for instance by developing a greedy/pruning scheme [13] or by improving a Monte Carlo tree search method [14].

The other class of sensor planning problems, the trajectory planning of mobile sensors, aims to optimize a sequence of waypoints/control inputs of sensor platforms to reduce the uncertainty of the target states. Mobile sensors offer distinctive advantages over static sensors in terms of the quality of sensing and estimation [3]–[6], [9], [17]–[20], area coverage, data offloading [22], the ability to change conditions of environments [8] as well as the target behavior. In this problem, not only the dynamics of the sensor platform but disturbances such as wind can also be considered for planning. One approach to solving this problem is to extend the method developed for sensor scheduling purposes. Decision variables, such as selecting the sensor in the sensor scheduling problem, can be treated in the same way as variables such as the control input of the mobile sensor [16], [17], [21]. However, this approach entails the computation time problem that occurs in sensor scheduling and requires an algorithm such as branch-and-bound based pruning [17]. Furthermore, because the control input has to be discretized, the dimension of the problem increases rapidly for sophisticated control of the sensor platform. Another approach is based on game/information theory to control mobile sensor networks [6]. That approach employs a particle filter for the purpose of estimating the state of the target more precisely when the stochastic dynamics of the target

is non-Gaussian and nonlinear, and it requires discretization of the control inputs. Accordingly, it is difficult to use in multi-step ahead planning. A local trajectory optimization method may be more suitable for the non-myopic planning of mobile sensors, as opposed to discretizing the control inputs and obtaining optimal solutions through algorithms such as a tree search. Many studies have performed trajectory optimization based on the gradient of the control inputs to a given objective function using analytically differentiable filter models [3], [4], [8], [9], [19]. Such formulations have a great advantage in handling the dynamic constraints of the sensor platform and/or environment. For instance, a trajectory planning method that takes into account the effects of wind on the sensor platform and collision avoidance was proposed [8]. Oshman et al. investigated optimal trajectory planning subject to state constraints imposed on the sensor platform [4]. Ponda et al. [3] used an FIM to quantify the amount of information acquired by sensor measurements and analyzed an optimality criterion for a bearings-only target localization problem.

For trajectory planning of sensor platforms in multi-target tracking problems, local trajectory optimization methods can easily become trapped in a local optimum unless the values of the optimization variables are not initialized appropriately. This calls for a high-level decision-making process before trajectory optimization. Specifically, decision-making should determine which mobile sensors should track which targets and in what order the targets should be tracked. This is also referred to as a task-assignment problem. Unfortunately, it is not easy to assign tasks, that is, to initialize optimization variables to the appropriate values, because the uncertainty of the target involved in the cost function of the problem depends not only on time but also on the dynamics of the sensor platforms and the target. A naive way of handling the task-assignment problem for multi-target tracking is to use an objective function of the problem at a specific time, or an intuitive value such as distance. As the number of targets increases, the task of assigning mobile sensors to targets in real-time becomes increasingly complex, as the states of both mobile sensors and targets change rapidly. To overcome such a computational challenge, most existing works adopt a two-phase approach to assigning tasks through the clustering of targets, after which they perform trajectory planning [5], [18], [23]. The targets are assumed to be static, and data mining tools such as the K-mean clustering algorithm or density-based spatial clustering of applications with noise (DBSCAN) [24] are used to form clusters based on the distance separating the targets. Clusters with large uncertainties or large numbers of targets are designated with higher priority over others for mobile sensor assignments. Tasks are assigned to mobile sensors based on the priority of the clusters and the distance between the mobile sensors and the center of the clusters. Then, one or two step trajectory planning is performed [5], [18]. Such myopic planning, however, can become trapped in the local optima and will perform poorly in some cases, such as planning with sensing holes [21], [25]. Although a sampling-based trajectory plan-

ning algorithm called the Information-rich Rapidly-exploring Random Tree (IRRT) algorithm [26] has been used for multi-step planning in [23], it does not guarantee any optimality.

On the other hand, the alternating direction method of multipliers (ADMM) [27]–[29] has been effectively applied to large-scale problems and to robotic control and sensor scheduling [30]–[34]. For instance, work by Liu et al. [34] considers the problem of finding optimal time-periodic sensor schedules for estimating the state of discrete-time dynamical systems. The problem is formulated to strike a balance between estimation accuracy and the total number of sensor activations over one period. They used ADMM to solve the optimization problem, including cardinality functions. Bento et al. [31] adopted ADMM for multi-agent trajectory planning. ADMM is used to efficiently solve a problem that involves different constraint and objective functions, such as collision avoidance and energy minimization. Ong et al. [30] also developed a message-passing algorithm based on ADMM to solve a cooperative collision avoidance problem. Mordatch et al. [33] combined trajectory optimization and global policy (neural network) learning using ADMM in a robotic control problem. The joint optimization problem enables the trajectory optimizer to act as a teacher for neural network training rather than as a demonstrator.

In this paper, we investigate informative trajectory planning for multi-target tracking problems. Existing local trajectory optimization-based algorithms focus on the non-myopic planning of mobile sensors rather than solving task-assignment problems [3], [4], [8], [9], [19]. In contrast, two-phase approaches were developed for the purpose of scalable task assignment rather than non-myopic trajectory planning [5], [18]. Such approaches approximate the original cost function or use intuitive values that can be indirectly related to the estimation performance for task assignment. Thus, they can provide a local optimal solution even for myopic trajectory planning problems [5]. Moreover, two-phase approaches use the information about the targets at the planning time to assign tasks, making them unsuitable for non-myopic trajectory planning problems that require consideration of changes in target states over time and mobile platform mobility. This work aims to bridge the gap between preliminary work on non-myopic trajectory planning [3], [4], [8], [9], [19] and task assignment [5], [18], [23]. In the trajectory planning problem for multiple target tracking, it is necessary to determine which mobile sensors should track which targets, in what order the targets should be tracked, and how much time should be devoted to each target. To the best of our knowledge, no attempt has been made to handle both non-myopic trajectory planning and task assignment in multi-target tracking problems simultaneously while considering the constraints of the sensor platform mobility and changes in target states over time.

The main contribution of this paper is two-fold. First, we propose a new informative trajectory planning algorithm for multi-target tracking problems which combines a local trajectory optimization method and ADMM. To circumvent solving task-assignment problem, which is difficult even to

configure in the non-myopic trajectory planning problem, we reconstruct the trajectory optimization problem for multi-target tracking as a trajectory optimization problem for each target and use ADMM to couple subproblems for each target. Coupling based on ADMM not only enables the results of each subproblem to be reflected in the trajectory optimization process of the other subproblems, but also guides the results of the subproblems to converge to the same solution. Specifically, the trajectories resulting from the subproblems for each target are deformed to improve the estimation performances of the target as well as the overall target during the specified planning horizon. In the process, the targets are automatically assigned to the mobile sensors. Consequently, our distributed framework enables decision making to be integrated into the trajectory optimization process, which means that task assignment and non-myopic trajectory planning problems can be solved simultaneously without the aid of task-assignment algorithm. Within our distributed framework, we use a second-order local trajectory optimization method to optimize the trajectory, as this method is known to be more stable and faster than the first-order local trajectory optimization method commonly used for trajectory planning. We also devise an initial guess generator for fixed-wing Unmanned Aerial Vehicle (UAV) dynamics with directional sensors to improve the solution quality and convergence speed of the local trajectory optimization algorithm. Second, we propose a receding-horizon control (RHC) scheme and an edge-cutting method for real-time implementation of the proposed algorithm. Our RHC scheme makes it possible to plan the future trajectory while taking into account the computation time of the trajectory optimization algorithm, which includes motion estimations of the targets. The edge-cutting method serves to reduce the dimensions of the subproblems during the optimization process. If the tuning parameters are set appropriately, the edge-cutting method reduces the computation time of the algorithm while yielding the same result as not applied.

The rest of this paper is organized as follows. In Section II, we define the trajectory optimization problem for multi-target tracking and reformulate the original problem as a distributed trajectory optimization problem. Section III presents the details of our algorithm; we describe the mathematical formulation of the distributed trajectory optimization algorithm. Convergence and computational complexity are analyzed in Section III-B. For rapid convergence of a solution, an edge-cutting method suitable for the multi-target tracking problem is developed in Section III-C. A receding-horizon control scheme is proposed for real-time implementation of the proposed algorithm in consideration of the computation time in Section III-D. Finally, simulation results of the proposed algorithms are given in Section IV.

II. PROBLEM DESCRIPTION AND PRELIMINARY

We begin by defining the trajectory optimization problem of mobile sensors to enhance the tracking performance. The goal of a target tracking problem is to estimate the kinematic states of targets with a finite set of measurements, which

naturally fits into Bayesian state estimation formulation (i.e., Bayesian filtering). Bayesian filtering formulation provides us with a measure for evaluation of the tracking performance. This measure represents the uncertainty of the target states, and the location of the mobile sensors should be planned to reduce it, that is, to enhance the tracking performance, over a specified time horizon. First, we present the mobile sensor and target models for the sake of concreteness. These models are used to define the trajectory planning problem of mobile sensors. Then, we formulate the distributed trajectory optimization for the multi-target tracking problem.

A. Mobile Sensor and Target Models

We consider the problem of multiple mobile sensors tracking multiple targets in the region of interest. Let a set of targets be represented as $\mathcal{T} = \{1, 2, \dots, M\}$. Here, we assume that the number of targets is known and fixed as M . If the targets move independently and the states of each target can be distinguished from others via data association methods [35], the joint distribution can be ignored and a single tracking filter can be used for each target [19]. Based on this assumption, we use linear stochastic dynamics for the state estimation of each target:

$$\mathbf{x}_{t+1}^{(j)} = A_t^{(j)} \mathbf{x}_t^{(j)} + \omega_t^{(j)}, \quad (1)$$

where $\omega_t^{(j)} \sim \mathcal{N}(0, \Sigma_{w,t}^{(j)})$ is the Gaussian random noise which is independent of other targets and measurements. $A_t^{(j)}$ and $\Sigma_{w,t}^{(j)}$ are the transition models of the target and process noise covariance, respectively. In this work, the motion of a target in a two-dimensional space is assumed to be modeled by the following matrices:

$$A_t^{(j)} = \begin{bmatrix} 1 & 0 & dt & 0 \\ 0 & 1 & 0 & dt \\ 0 & 0 & 1 & 0 \\ 0 & 0 & 0 & 1 \end{bmatrix}, Q_t^{(j)} = q \begin{bmatrix} \frac{dt^3}{3} & 0 & \frac{dt^2}{2} & 0 \\ 0 & \frac{dt^3}{3} & 0 & \frac{dt^2}{2} \\ \frac{dt^2}{2} & 0 & dt & 0 \\ 0 & \frac{dt^2}{2} & 0 & dt \end{bmatrix}, \quad (2)$$

where dt is the time interval between two successive measurements, and q is the process noise intensity representing the strength of the deviations from the predicted motion by the dynamic model [36]. When q is small, this model represents a nearly constant velocity.

Let $\mathcal{P} \subset \mathbb{R}^n$ and $\mathcal{U} \subset \mathbb{R}^c$ be the state space and the control input space of the mobile sensors, respectively, and let a set of mobile sensors be represented as $\mathcal{A} = \{1, 2, \dots, N\}$. The corresponding dynamics can then be expressed as:

$$p_{t+1}^{(i)} = f^{(i)}(p_t^{(i)}, u_t^{(i)}), \quad (3)$$

where $p_t^{(i)} \in \mathcal{P}^{(i)}$, $u_t^{(i)} \in \mathcal{U}^{(i)}$, and $i \in \mathcal{A}$ are the state and control input of the mobile sensor at time t and index for the mobile sensors, respectively. For sensor platforms, we consider a set of fixed-wing Unmanned Aerial Vehicles

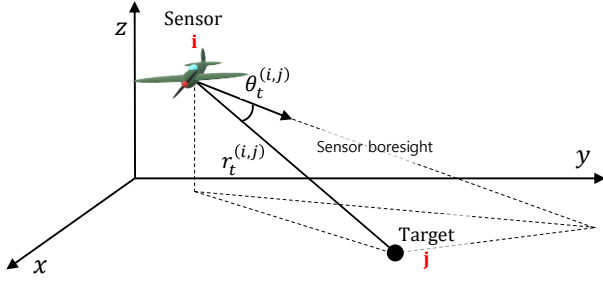


Fig. 1: Sensor model for target tracking

(UAVs). The dynamics of the UAVs is given by:

$$\begin{aligned}
 p_{x,t+1}^{(i)} &= p_{x,t}^{(i)} + V^{(i)} \cos \psi_t^{(i)} dt, \\
 p_{y,t+1}^{(i)} &= p_{y,t}^{(i)} + V^{(i)} \sin \psi_t^{(i)} dt, \\
 \psi_{t+1}^{(i)} &= \psi_t^{(i)} + g \tan \phi_t^{(i)} dt / V^{(i)}, \\
 \phi_{t+1}^{(i)} &= \phi_t^{(i)} + u_t^{(i)} dt,
 \end{aligned} \tag{4}$$

where $[p_x^{(i)}, p_y^{(i)}]$, $V^{(i)}$, $\psi_t^{(i)}$ and $\phi^{(i)}$ are the position, speed, heading angle and bank angle of i -th UAV, respectively. Gravity acceleration is denoted as g . Sensors are assumed to measure the kinematic information about the target relative to the sensor, itself.

Let $\mathcal{Z} \subset \mathbb{R}^o$ be the space of all possible sensor measurements that the mobile sensors receive. Each UAV is assumed to be equipped with one sensor for simplicity.¹ Denoting the measurement taken by the i -th UAV from target j at time t as $z_t^{(i,j)} \in \mathcal{Z}^{(i)}$, a nonlinear measurement model is assumed as follows:

$$z_t^{(i,j)} = h^{(i)}(\mathbf{x}_t^{(j)}, p_t^{(i)}) + v_t^{(i)}, \tag{5}$$

where $v_t^{(i)} \sim \mathcal{N}(0, \Sigma_{v,t}^{(i)})$ is the Gaussian random noise, independent of the other measurement noises and of the process noise $u_t^{(i)}$. Each sensor measures the signal-to-noise ratio (SNR) [37]:

$$h^{(i)}(\mathbf{x}_t^{(j)}, p_t^{(i)}) = \frac{\alpha e^{-\gamma (\theta_t^{(i,j)})^2}}{(r_t^{(i,j)}) + \beta}, \tag{6}$$

where α , β , and γ are selected to model the SNR of the sensor. $r_t^{(i,j)}$ and $\theta_t^{(i,j)}$ represent the distance between the sensor and the target as well as the angle between the sensor's boresight and the direction from the sensor to the target, respectively. When γ is set to zero, the sensor measures the quasi-distance, which is a commonly used model [6], [13], [38]. The sensors are assumed to be mounted at the left or the right side of the UAVs and aim down (Fig. 1).

¹ In this paper, we use a term 'mobile sensor' and 'UAV' interchangeably. For simplicity, we assume that each UAV has one sensor on it. In general, some platforms can carry more than one sensor, and the sensors can be heterogeneous. In such cases, the sensing locations for the sensors on the same vehicle should match, and the measurement $z_t^{(i,j)}$ of the i -th UAV for each target j increases in proportion to the number of sensors.

B. Estimation

Given the current belief states of the targets $(\hat{\mathbf{x}}_t^{(j)}, \Sigma_t^{(j)})$, the states of the mobile sensors $\mathbf{p}_t = [p_t^{(1)\top}, \dots, p_t^{(N)\top}]^\top$ and the measurements $\mathbf{z}_t^{(j)} = [z_t^{(1,j)\top}, \dots, z_t^{(N,j)\top}]^\top$, we let the belief evolve using the extended Kalman filter (EKF). The EKF is widely used for state estimation of non-linear systems [39], which is applicable to Gaussian beliefs. Note that any other non-linear Gaussian filter, such as an unscented Kalman filter, can be incorporated instead. For notational simplicity, we temporarily drop the subscript (j) . The EKF update equations are then given by:

$$\hat{\mathbf{x}}_{t+1} = A_t \hat{\mathbf{x}}_t + K_t (\mathbf{z}_{t+1} - \mathbf{h}_t(\hat{\mathbf{x}}_{t+1}, \mathbf{p}_{t+1})), \tag{7}$$

$$\Sigma_{t+1} = (I - K_t H_t) \bar{\Sigma}_t, \tag{8}$$

where

$$\bar{\Sigma}_t = A_t \Sigma_t A_t^T + \Sigma_{w,t},$$

$$K_t = \bar{\Sigma}_t H_t^T (H_t \bar{\Sigma}_t H_t^T + \Sigma_{v,t})^{-1},$$

$$\Sigma_{v,t} = \text{diag}([\Sigma_{v,t}^{(1)}, \dots, \Sigma_{v,t}^{(N)}]),$$

$$H_t = \left. \frac{\partial \mathbf{h}(\mathbf{x}_t, \mathbf{p}_t)}{\partial \mathbf{x}_t} \right|_{\hat{\mathbf{x}}_t, \mathbf{p}_t},$$

$$\mathbf{h} = [h^{(1)}(\mathbf{x}_t, p_t), \dots, h^{(N)}(\mathbf{x}_t, p_t)]^\top.$$

Equations (7) and (8) define the belief dynamics. The second term in (7), called the innovation term, depends on the measurements \mathbf{z}_{t+1} . Equation (8) evolves given the current covariance of the target, regardless of the measurement. This represents the uncertainty of the target states and can be used as a measure to determine the sensing position of the mobile sensors. Because the measurement is unknown in advance, the belief dynamics defined within the EKF update is stochastic; the innovation term is distributed according to $\mathcal{N}(0, K_t H_t \bar{\Sigma}_t)$ [40].

We define the belief states of the j -th target as $\mathbf{b}_t^{(j)} = [\hat{\mathbf{x}}_t^{(j)\top}, \text{vec}[\Sigma_t^{(j)}]^\top]^\top$ and $\text{vec}[\cdot]$ returns a vector consisting of the symmetric elements of a matrix since $\Sigma_t^{(j)}$ is symmetric. Then, the stochastic belief dynamics of the target is given by:

$$\mathbf{b}_{t+1} = \mathbf{g}(\mathbf{b}_t, \mathbf{p}_t) + \psi_t, \quad \psi_t \sim \mathcal{N}(0, \Psi), \tag{9}$$

where

$$\mathbf{g}(\mathbf{b}_t, \mathbf{p}_t) = \begin{bmatrix} A_t \hat{\mathbf{x}}_t \\ \text{vec}[(I - K_t H_t) \bar{\Sigma}_t] \end{bmatrix}, \tag{10}$$

$$\Psi(\mathbf{b}_t, \mathbf{p}_t) = \text{Var}[\mathbf{b}_{t+1}] = \begin{bmatrix} K_t H_t \bar{\Sigma}_t & 0 \\ 0 & 0 \end{bmatrix}.$$

Here, if we assume maximum-likelihood observations [41], the stochastic term is removed from (9), which makes belief propagation deterministic.

C. Distributed Trajectory Optimization Problem

In the target tracking problem, the performance metric is represented by a function of the covariance structure and has various forms according to the objective. We chose the trace of the error covariance matrix as the performance metric.

The trace is one of the most commonly used metrics. Note that any differentiable metric can be incorporated instead. Given a specific initial state and target uncertainty, one can find an optimal trajectory $[\mathbf{P}, \mathbf{U}]$ that satisfies the dynamics constraints:

$$[\bar{\mathbf{P}}, \bar{\mathbf{U}}] = \underset{\mathbf{p}, \mathbf{u}}{\operatorname{argmin}} \sum_{t=0}^T \left[\sum_{j=1}^M \operatorname{tr}(Q\Sigma_t^{(j)}(\mathbf{p}_t)) \right] + \mathbf{u}_t^\top R \mathbf{u}_t + \eta(\mathbf{p}_t), \quad (11)$$

subject to

$$\mathbf{p}_{t+1} = \mathbf{f}(\mathbf{p}_t, \mathbf{u}_t), \quad \mathbf{b}_{t+1}^{(j)} = \mathbf{g}(\mathbf{b}_t^{(j)}, \mathbf{p}_t) + \psi_t^{(j)},$$

$$\mathbf{p}_0 = \mathbf{p}_{init} \quad \text{and} \quad \mathbf{b}_0^{(j)} = \mathbf{b}_{init}^{(j)},$$

where

$$\mathbf{f}(\mathbf{p}_t, \mathbf{u}_t) = \left[f^{(1)}(p_t^{(1)}, u_t^{(1)})^\top, \dots, f^{(N)}(p_t^{(N)}, u_t^{(N)})^\top \right]^\top,$$

$$\mathbf{p}_t = \left[p_t^{(1)\top}, \dots, p_t^{(N)\top} \right]^\top, \quad \mathbf{u}_t = \left[u_t^{(1)\top}, \dots, u_t^{(N)\top} \right]^\top.$$

$\operatorname{tr}[Q\Sigma_t^{(j)}(\cdot)]$ is the uncertainty of the j -th target at time t , $\mathbf{u}_t^\top R \mathbf{u}_t$ penalizes the control effort of the mobile sensors along the trajectory, and $\eta(\mathbf{X}_t)$ is a function related to the states of the mobile sensors. Q and R are weighting matrices. The problem defined in (11) is a general trajectory optimization problem for a stochastic system. The states of the mobile sensors \mathbf{p} are associated with the covariance matrix representing the uncertainty of the target Σ via Bayesian estimation in Equations (8) and (9). Thus, the planning objective is to optimize a sequence of states/control inputs of mobile sensors over a certain future time step T to minimize the uncertainty of the targets.

In the trajectory optimization problem (11), there exist numerous local optimal solutions due to the non-convexity of the cost function. This non-convexity is primarily because the optimal sensor trajectories can be significantly different depending on which target is assigned to which sensor. Therefore, we need to guide a solution by properly initializing the optimization variables. Initialized optimization variables are called an initial guess. The solutions of most trajectory optimization methods are basically generated around an initial guess for the region where the cost gradient and/or Hessian exists, and the initial guess can be interpreted as having a role similar to task assignment in a multi-target tracking problem. Unfortunately, constructing a task-assignment problem is very difficult because the cost function (11) depends not only on the time but also on the states of the mobile sensors and targets. To overcome this difficulty, we reformulate the original problem (11) into a distributed trajectory optimization problem for each target:

$$[\bar{\mathbf{P}}, \bar{\mathbf{U}}] = \underset{\mathbf{u}}{\operatorname{argmin}} \sum_{j=1}^M \mathbf{J}_j(\mathbf{P}, \mathbf{U}), \quad (12)$$

subject to

$$\mathbf{p}_{t+1} = \mathbf{f}(\mathbf{p}_t, \mathbf{u}_t), \quad \mathbf{b}_{t+1}^{(j)} = \mathbf{g}(\mathbf{b}_t^{(j)}, \mathbf{p}_t) + \psi_t^{(j)},$$

$$\mathbf{p}_0 = \mathbf{p}_{init} \quad \text{and} \quad \mathbf{b}_0^{(j)} = \mathbf{b}_{init}^{(j)},$$

where

$$\mathbf{J}_j(\mathbf{P}, \mathbf{U}) = \sum_{t=0}^T \operatorname{tr}(Q\Sigma_t^{(j)}(\mathbf{p}_t)) + \frac{1}{M} (\mathbf{u}_t^\top R \mathbf{u}_t + \eta(\mathbf{p}_t)),$$

$$\mathbf{P} = [\mathbf{p}_1, \dots, \mathbf{p}_T], \quad \mathbf{U} = [\mathbf{u}_1, \dots, \mathbf{u}_T].$$

Trajectory optimization for each target is relatively easier than that for multiple targets because task assignment does not need to be considered. That is, it is not difficult to generate the initial guess for the problem of tracking each target. The trajectory optimization results for each subproblem must be reflected in the optimization of each of the other subproblems and the results must converge to the same solution. To do this, we adopt the Alternating Direction Method of Multipliers (ADMM) method [27], [42].

D. Distributed Alternating Direction Method of Multipliers

ADMM is an algorithm that efficiently optimizes objective functions composed of terms that each have efficient solution methods [27]. For our purposes, we use a consensus and sharing optimization form of the Alternating Direction Method of Multipliers (ADMM) method, also known as distributed-ADMM [28], [29], [42]. We consider the following minimization problem:

$$\min \sum_{l=1}^L J_l(a). \quad (13)$$

This problem can be rewritten with the local variable a_l and common global variable b :

$$\min \sum_{l=1}^L J_l(a_l), \quad \text{s.t.} \quad a_l - b = 0, \quad l = 1, \dots, L. \quad (14)$$

This is called the *global consensus problem*, as the constraint is that all the local variables should be equal (i.e., agree). Solving this problem is equivalent to optimizing the augmented Lagrangian:

$$\mathcal{L}(\lambda_l) = \sum_{l=1}^L (J_l(a_l) + \frac{\rho}{2} \|a_l - b + \lambda_l\|^2), \quad (15)$$

where λ_l is the Lagrange multipliers for $a_l - b = 0$, and $\rho > 0$ is a penalty weight. The ADMM algorithm updates the local variable a_l , the common global variable b and the Lagrange multiplier λ_l as follows. For $k = 0, 1, \dots$, we iteratively execute the following three steps:

$$a_l^{k+1} = \underset{a_l}{\operatorname{argmin}} J_l(a_l) + \frac{\rho}{2} \|a_l - b^k + \lambda_l^k\|^2,$$

$$b^{k+1} = \frac{1}{L} \sum_{l=1}^L (a_l^{k+1} + \lambda_l^k), \quad (16)$$

$$\lambda_l^{k+1} = \lambda_l^k + \frac{\alpha}{\rho} (a_l^{k+1} - b^{k+1}),$$

where $\alpha > 0$ is a step-size parameter. Here, the first and the last steps can be carried out independently for each $l = 1, \dots, L$. At this point, we can run distributed or parallel ADMM depending on the implementation with multiple but no more than L computational devices, where each device

performs an update on its set of variables. The optimization results a_l are communicated back to a master node, which performs the global variable b update and returns the result back to other worker nodes. The processing element that handles the global variable b is sometimes called the central collector or the fusion center.

III. ALGORITHM DESCRIPTION

We now describe the distributed trajectory optimization algorithm to solve problem (12). For the trajectory optimization problem for each target j , we define the states and control inputs of the mobile sensor as \mathbf{p}_j and \mathbf{u}_j , respectively. These correspond to states and control inputs that need to be optimized to minimize the uncertainty of each target. The augmented Lagrangian for problem (12) is defined as follows:

$$\begin{aligned} \mathcal{L}(\mathbf{P}^\lambda, \mathbf{U}^\lambda) = & \sum_{j=1}^M \mathbf{J}_j(\mathbf{P}_j, \mathbf{U}_j) + \frac{\rho_v}{2} \|\mathbf{P}_j - \mathbf{P}^C + \mathbf{P}_j^\lambda\|^2 \\ & + \frac{\rho_u}{2} \|\mathbf{U}_j - \mathbf{U}^C + \mathbf{U}_j^\lambda\|^2, \end{aligned} \quad (17)$$

subject to

$$\begin{aligned} \mathbf{p}_{j,t+1} = & \mathbf{f}(\mathbf{p}_{j,t}, \mathbf{u}_{j,t}), \quad \mathbf{b}_{t+1}^{(j)} = \mathbf{g}(\mathbf{b}_t^{(j)}, \mathbf{p}_{j,t}) + \boldsymbol{\psi}_t^{(j)}, \\ \mathbf{p}_{j,0} = & \mathbf{p}_{j,init} \quad \text{and} \quad \mathbf{b}_0^{(j)} = \mathbf{b}_{init}^{(j)}. \end{aligned}$$

Each of the variables is updated in a distributed manner, as described in Section II-D.

The update for the trajectory variables for each target j is:

$$\begin{aligned} [\bar{\mathbf{P}}_j, \bar{\mathbf{U}}_j] = & \underset{\mathbf{P}, \mathbf{U}}{\operatorname{argmin}} \sum_{t=0}^T \operatorname{tr}(Q\Sigma_t^{(j)}(\mathbf{p}_t)) \\ & + \frac{1}{M} (\mathbf{u}_t^\top R \mathbf{u}_t + \eta(\mathbf{p}_t)) + \frac{\rho_v}{2} \|\mathbf{p}_t - \mathbf{P}_t^C + \mathbf{P}_{j,t}^\lambda\|^2 \\ & + \frac{\rho_u}{2} \|\mathbf{u}_t - \mathbf{U}_t^C + \mathbf{U}_{j,t}^\lambda\|^2, \end{aligned} \quad (18)$$

subject to

$$\begin{aligned} \mathbf{p}_{t+1} = & \mathbf{f}(\mathbf{p}_t, \mathbf{u}_t), \quad \mathbf{b}_{t+1}^{(j)} = \mathbf{g}(\mathbf{b}_t^{(j)}, \mathbf{p}_t) + \boldsymbol{\psi}_t^{(j)}, \\ \mathbf{p}_0 = & \mathbf{p}_{init} \quad \text{and} \quad \mathbf{b}_0^{(j)} = \mathbf{b}_{init}^{(j)}. \end{aligned}$$

This is a trajectory optimization problem with two additional quadratic cost terms and can be solved with the existing trajectory optimization methods described in Section III-A. The trajectory optimization problems for each target j are independent and can be solved in parallel.

The updates for the common global variables are as follows:

$$\begin{aligned} \mathbf{P}^C = & \frac{1}{M} \sum_{j=1}^M (\bar{\mathbf{P}}_j + \mathbf{P}_j^\lambda), \\ \mathbf{U}^C = & \frac{1}{M} \sum_{j=1}^M (\bar{\mathbf{U}}_j + \mathbf{U}_j^\lambda). \end{aligned} \quad (19)$$

This is the mean consensus process that takes the average of the results for each trajectory optimization. The common global variables again affect the update of the trajectory

Algorithm 1 Distributed Trajectory Optimization

- 1: Choose penalty weight ρ and step-size α
 - 2: Generate initial guess $[\mathbf{P}_j, \mathbf{U}_j]$ for each target j
 - 3: Initialize trajectory optimization solutions with $[\mathbf{P}_j, \mathbf{U}_j]$
 - 4: **while** not converged **do**
 - 5: Update $[\mathbf{P}_j, \mathbf{U}_j]$ by solving each trajectory optimization problems (18) in parallel (see Section III-A)
 - 6: Update $[\mathbf{P}^C, \mathbf{U}^C]$ by averaging the results for each trajectory optimization
 - 7: Update $[\mathbf{P}^\lambda, \mathbf{U}^\lambda]$ using (20)
 - 8: **end while**
-

variables for each target j (18), which causes the results of trajectory optimization for each target to converge to the same solution.

The updates for the Lagrange multipliers are as follows:

$$\begin{aligned} \mathbf{P}_j^\lambda = & \mathbf{P}_j^\lambda + \frac{\alpha_v}{\rho_v} (\bar{\mathbf{P}}_j - \mathbf{P}^C), \\ \mathbf{U}_j^\lambda = & \mathbf{U}_j^\lambda + \frac{\alpha_u}{\rho_u} (\bar{\mathbf{U}}_j - \mathbf{U}^C), \quad \forall j. \end{aligned} \quad (20)$$

λ plays a role in giving more weight to regions where the difference between the global variables and the trajectory variables is large. As the process described above is repeated, λ changes the cost of the trajectory optimization problem in (18). Over time, this has the effect of modifying the optimal trajectory solutions and trajectory variables are guided into more informative regions, where tasks are automatically assigned so that mobile sensors can further reduce the uncertainty of the targets. Thus, λ can be seen as an alternative to high-level decision-making. The complete procedure is summarized in Algorithm 1.

A. Trajectory Optimization

We adopt belief space iterative Linear Quadratic Gaussian (belief space iLQG [40]) to solve the trajectory optimization problems described in (18). Belief space iLQG extends the iLQG method [43] to Partially Observable Markov Decision Processes (POMDPs) using a Gaussian belief, instead of a fully observable state. In the forward pass, belief space iLQG uses a standard extended Kalman filter (EKF) to compute the next time step belief. For a backward pass, belief space iLQG linearizes covariance in addition to quadratizing states and control inputs. Although the application of this approach is focused on the control problems of the system, it is directly applicable to the estimation problem (i.e., target tracking problem) due to the duality of control and estimation.

The belief dynamics of the target is given in (9), and by integrating it with the dynamics of mobile sensors, the entire system can be represented by:

$$\mathbf{v}_{t+1} = \mathcal{F}(\mathbf{v}_t, \mathbf{u}_t) + \mathbf{w}_t, \quad \mathbf{w}_t \sim \mathcal{N}(0, W), \quad (21)$$

where

$$\mathbf{v}_t = \begin{bmatrix} \mathbf{b}_t \\ \mathbf{p}_t \end{bmatrix}, \quad \mathcal{F}(\mathbf{v}_t) = \begin{bmatrix} \mathbf{g}(\mathbf{b}_t, \mathbf{p}_t) \\ \mathbf{f}(\mathbf{p}_t, \mathbf{u}_t) \end{bmatrix}, \quad W = \begin{bmatrix} \Psi & 0 \\ 0 & 0 \end{bmatrix}.$$

1) *Control Policy*: By linearizing the dynamics around the nominal trajectory distribution, the approximate dynamics is expressed as:

$$\begin{aligned} \mathbf{v}_{t+1} - \bar{\mathbf{v}}_{t+1} &\approx \mathcal{F}_{\mathbf{v},t}(\mathbf{v}_t - \bar{\mathbf{v}}_t) + \mathcal{F}_{\mathbf{u},t}(\mathbf{u}_t - \bar{\mathbf{u}}_t), \\ W_{(i)}(\mathbf{v}_t, \mathbf{u}_t) &\approx \mathbf{e}_t^i + \mathcal{F}_{\mathbf{v},t}^{(i)}(\mathbf{v}_t - \bar{\mathbf{v}}_t) + \mathcal{F}_{\mathbf{u},t}^{(i)}(\mathbf{u}_t - \bar{\mathbf{u}}_t), \end{aligned} \quad (22)$$

where

$$\begin{aligned} \mathcal{F}_{\mathbf{v},t} &= \frac{\partial \mathcal{F}}{\partial \mathbf{v}}(\bar{\mathbf{v}}_t, \bar{\mathbf{u}}_t), \quad \mathcal{F}_{\mathbf{u},t} = \frac{\partial \mathcal{F}}{\partial \mathbf{u}}(\bar{\mathbf{v}}_t, \bar{\mathbf{u}}_t), \\ \mathbf{e}_t^i &= W_{(i)}(\bar{\mathbf{v}}_t, \bar{\mathbf{u}}_t), \quad \mathcal{F}_{\mathbf{v},t}^i = \frac{\partial W_{(i)}}{\partial \mathbf{v}}(\bar{\mathbf{v}}_t, \bar{\mathbf{u}}_t), \\ \mathcal{F}_{\mathbf{u},t}^i &= \frac{\partial W_{(i)}}{\partial \mathbf{u}}(\bar{\mathbf{v}}_t, \bar{\mathbf{u}}_t). \end{aligned}$$

$W_{(i)}(\mathbf{v}_t, \mathbf{u}_t)$ is the i -th column of matrix $W(\mathbf{v}_t, \mathbf{u}_t)$. Note that $W_{(i)}(\mathbf{v}_t, \mathbf{u}_t)$ has n columns, where n is the dimension of the state. For a general nonquadratic cost function (18), we approximate it as a quadratic function along the nominal belief and control trajectory $(\bar{\mathbf{v}}, \bar{\mathbf{u}})$. For the notional simplicity, the cost function (18) is denoted by $\ell(\mathbf{v}_t, \mathbf{u}_t)$,

$$\begin{aligned} \ell(\mathbf{v}_t, \mathbf{u}_t) &\approx \frac{1}{2} \begin{bmatrix} \delta \mathbf{v}_t \\ \delta \mathbf{u}_t \end{bmatrix}^\top \begin{bmatrix} \ell_{\mathbf{v}\mathbf{v},t} & \ell_{\mathbf{v}\mathbf{u},t} \\ \ell_{\mathbf{u}\mathbf{v},t} & \ell_{\mathbf{u}\mathbf{u},t} \end{bmatrix} \begin{bmatrix} \delta \mathbf{v}_t \\ \delta \mathbf{u}_t \end{bmatrix} \\ &+ \begin{bmatrix} \delta \mathbf{v}_t \\ \delta \mathbf{u}_t \end{bmatrix}^\top \begin{bmatrix} \ell_{\mathbf{v},t} \\ \ell_{\mathbf{u},t} \end{bmatrix} + \ell_{0,t}, \end{aligned} \quad (23)$$

where $\ell_{0,t} = \ell(\bar{\mathbf{v}}_t, \bar{\mathbf{u}}_t)$. $\delta \mathbf{v}_t = \mathbf{v}_t - \bar{\mathbf{v}}_t$, $\delta \mathbf{u}_t = \mathbf{u}_t - \bar{\mathbf{u}}_t$ are deviations from the nominal trajectory and the terms with subscripts denote Jacobian and Hessian matrices of their respective functions.

Given the linear dynamics (22) and quadratic cost (23), we can obtain a quadratic approximation of the value function along a nominal trajectory $\bar{\mathbf{v}}_t$:

$$\mathbf{V}_t(\mathbf{v}_t) \approx \frac{1}{2} \delta \mathbf{v}_t^\top \mathbf{V}_{\mathbf{v}\mathbf{v},t} \delta \mathbf{v}_t + \delta \mathbf{v}_t^\top \mathbf{V}_{\mathbf{v},t} + \mathbf{V}_{0,t}. \quad (24)$$

Following the dynamic programming principle [44], the Bellman equation for the value function $\mathbf{V}_t(\mathbf{v}_t)$ and control policy $\pi_t(\mathbf{v}_t)$ in discrete-time are specified as:

$$\begin{aligned} \mathbf{V}_t(\mathbf{v}_t) &= \min_{\mathbf{u}_t} \left(\ell(\mathbf{v}_t, \mathbf{u}_t) + \mathbb{E}[\mathbf{V}_{t+1}(\mathcal{F}(\mathbf{v}_t, \mathbf{u}_t) + \mathbf{w}_t)] \right) \\ &= \min_{\mathbf{u}_t} \left(\ell(\mathbf{v}_t, \mathbf{u}_t) + \frac{1}{2} \delta \mathbf{v}_{t+1}^\top \mathbf{V}_{\mathbf{v}\mathbf{v},t+1} \delta \mathbf{v}_{t+1} \right. \\ &\quad \left. + \delta \mathbf{v}_{t+1}^\top \mathbf{V}_{\mathbf{v},t+1} + \mathbf{V}_{0,t+1} \right. \\ &\quad \left. + \frac{1}{2} \text{tr}[W(\mathbf{v}_t, \mathbf{u}_t)^\top \mathbf{V}_{\mathbf{v}\mathbf{v},t+1} W(\mathbf{v}_t, \mathbf{u}_t)] \right) \\ &= \min_{\mathbf{u}_t} \mathbf{Q}(\mathbf{v}_t, \mathbf{u}_t), \\ \pi_t(\mathbf{v}_t) &= \underset{\mathbf{u}_t}{\text{argmin}} \left(\ell(\mathbf{v}_t, \mathbf{u}_t) + \mathbb{E}[\mathbf{V}_{t+1}(\mathcal{F}(\mathbf{v}_t, \mathbf{u}_t) + \mathbf{w}_t)] \right), \end{aligned} \quad (25)$$

where

$$\text{tr}[W(\mathbf{v}_t, \mathbf{u}_t)^\top \mathbf{V}_{\mathbf{v}\mathbf{v},t+1} W(\mathbf{v}_t, \mathbf{u}_t)] = \sum_{i=1}^m W_{(i)}(\mathbf{v}_t, \mathbf{u}_t).$$

By substituting equations (22) and (23) into (25), the \mathbf{Q} -function is given by:

$$\begin{aligned} \mathbf{Q}_t(\bar{\mathbf{v}}_t + \delta \mathbf{v}_t, \bar{\mathbf{u}}_t + \delta \mathbf{u}_t) &= \frac{1}{2} \begin{bmatrix} \delta \mathbf{v}_t \\ \delta \mathbf{u}_t \end{bmatrix}^\top \begin{bmatrix} \mathbf{Q}_{\mathbf{v}\mathbf{v},t} & \mathbf{Q}_{\mathbf{v}\mathbf{u},t} \\ \mathbf{Q}_{\mathbf{u}\mathbf{v},t} & \mathbf{Q}_{\mathbf{u}\mathbf{u},t} \end{bmatrix} \begin{bmatrix} \delta \mathbf{v}_t \\ \delta \mathbf{u}_t \end{bmatrix} \\ &+ \begin{bmatrix} \delta \mathbf{v}_t \\ \delta \mathbf{u}_t \end{bmatrix}^\top \begin{bmatrix} \mathbf{Q}_{\mathbf{v},t} \\ \mathbf{Q}_{\mathbf{u},t} \end{bmatrix} + \mathbf{Q}_{0,t}, \end{aligned} \quad (26)$$

where

$$\begin{aligned} \mathbf{Q}_{\mathbf{v}\mathbf{v},t} &= \ell_{\mathbf{v}\mathbf{v},t} + \mathcal{F}_{\mathbf{v},t}^\top \mathbf{V}_{\mathbf{v}\mathbf{v},t+1} \mathcal{F}_{\mathbf{v},t} + \sum_{i=1}^m \mathcal{F}_{\mathbf{v},t}^{i\top} \mathbf{V}_{\mathbf{v}\mathbf{v},t+1} \mathcal{F}_{\mathbf{v},t}^i, \\ \mathbf{Q}_{\mathbf{v},t} &= \ell_{\mathbf{v},t} + \mathcal{F}_{\mathbf{v},t}^\top \mathbf{V}_{\mathbf{v},t+1} + \sum_{i=1}^m \mathcal{F}_{\mathbf{v},t}^{i\top} \mathbf{V}_{\mathbf{v}\mathbf{v},t+1} \mathbf{e}_t^i, \\ \mathbf{Q}_{\mathbf{u}\mathbf{u},t} &= \ell_{\mathbf{u}\mathbf{u},t} + \mathcal{F}_{\mathbf{u},t}^\top \mathbf{V}_{\mathbf{v}\mathbf{v},t+1} \mathcal{F}_{\mathbf{u},t} + \sum_{i=1}^m \mathcal{F}_{\mathbf{u},t}^{i\top} \mathbf{V}_{\mathbf{v}\mathbf{v},t+1} \mathcal{F}_{\mathbf{u},t}^i, \\ \mathbf{Q}_{\mathbf{u},t} &= \ell_{\mathbf{u},t} + \mathcal{F}_{\mathbf{u},t}^\top \mathbf{V}_{\mathbf{v},t+1} + \sum_{i=1}^m \mathcal{F}_{\mathbf{u},t}^{i\top} \mathbf{V}_{\mathbf{v}\mathbf{v},t+1} \mathbf{e}_t^i, \\ \mathbf{Q}_{\mathbf{u}\mathbf{v},t} &= \ell_{\mathbf{u}\mathbf{v},t} + \mathcal{F}_{\mathbf{u},t}^\top \mathbf{V}_{\mathbf{v}\mathbf{v},t+1} \mathcal{F}_{\mathbf{v},t} + \sum_{i=1}^m \mathcal{F}_{\mathbf{u},t}^{i\top} \mathbf{V}_{\mathbf{v}\mathbf{v},t+1} \mathcal{F}_{\mathbf{v},t}^i, \\ \mathbf{Q}_{0,t} &= \ell_{0,t} + \mathbf{V}_{0,t+1} + \sum_{i=1}^n \mathbf{e}_t^{i\top} \mathbf{V}_{\mathbf{v}\mathbf{v},t+1} \mathbf{e}_t^i. \end{aligned} \quad (27)$$

In order to find the optimal control policy, we compute the local variations in the control $\delta \hat{\mathbf{u}}$ that minimize the quadratic approximation of the \mathbf{Q} -function in (25):

$$\begin{aligned} \delta \hat{\mathbf{u}}_t &= \underset{\delta \mathbf{u}_t}{\text{argmax}} [\mathbf{Q}_t(\bar{\mathbf{v}}_t + \delta \mathbf{v}_t, \bar{\mathbf{u}}_t + \delta \mathbf{u}_t)] \\ &= -\mathbf{Q}_{\mathbf{u}\mathbf{u},t}^{-1} \mathbf{Q}_{\mathbf{u},t} - \mathbf{Q}_{\mathbf{u}\mathbf{v},t}^{-1} \delta \mathbf{v}_t. \end{aligned} \quad (28)$$

The optimal control can be found as $\hat{\mathbf{u}}_t = \bar{\mathbf{u}}_t + \delta \hat{\mathbf{u}}_t$. Substituting (28) into (25) gives the value function $\mathbf{V}_t(\mathbf{v}_t)$ as a function of only \mathbf{v}_t in the form of (24):

$$\begin{aligned} \mathbf{V}_{\mathbf{v}\mathbf{v},t} &= \mathbf{Q}_{\mathbf{v}\mathbf{v},t} - \mathbf{Q}_{\mathbf{u}\mathbf{v},t}^\top \mathbf{Q}_{\mathbf{u}\mathbf{u},t}^{-1} \mathbf{Q}_{\mathbf{u}\mathbf{v},t}, \\ \mathbf{V}_{\mathbf{v},t} &= \mathbf{Q}_{\mathbf{v},t} - \mathbf{Q}_{\mathbf{u}\mathbf{v},t}^\top \mathbf{Q}_{\mathbf{u}\mathbf{u},t}^{-1} \mathbf{Q}_{\mathbf{u},t}, \\ \mathbf{V}_{0,t} &= \mathbf{Q}_{0,t} - \mathbf{Q}_{\mathbf{u},t}^\top \mathbf{Q}_{\mathbf{u}\mathbf{u},t}^{-1} \mathbf{Q}_{\mathbf{u},t}. \end{aligned} \quad (29)$$

This recursion then continues by computing the control policy for time step $t-1$.

2) *Initial Guess Generation*: In the local trajectory optimization, the initial guess has a great effect on the convergence speed as well as on the quality of the solution. Thus, it is very important to generate appropriate initial guesses for the purpose of the problem. To do this, we derive an initial guess generator for the target tracking problem based on a Dubins path [45] that can mimic the behavior of a fixed-wing UAV. Let $r_{min}^{(i)}$, $r_{sen}^{(i)}$ and $\hat{x}^{(j)}$ be the minimum turning radius of the i -th UAV, the distance between the i -th UAV's nadir point and the center point of the sensor footprint and the expected position of the target j , respectively. A path is created to arrive as soon as possible in a circle with radius $r_{sen}^{(i)}$ centered on the expected location $\hat{x}^{(j)}$ of the target j , and a path is added so that a sensor rotates in the direction

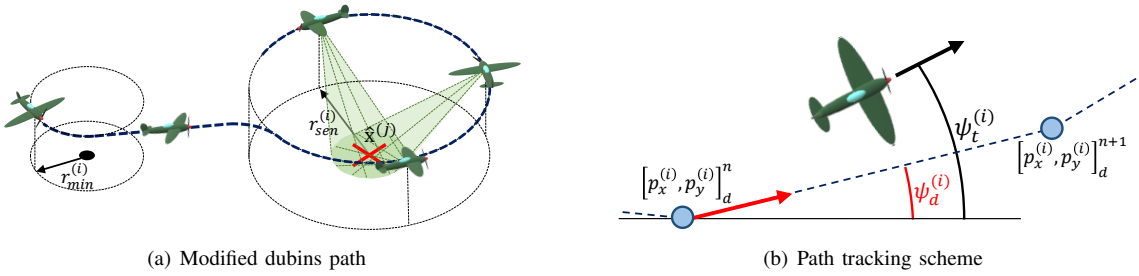


Fig. 2: The path is generated by a modified Dubins path algorithm, which is used to provide waypoints for the generation of the initial guess. Control inputs are generated so that UAV follows the path connecting the waypoints through the PD-controller, and these are used as the initial guess of the local trajectory optimization method.

facing the target. Here, $r_{sen}^{(i)}$ should be set to an appropriate value taking into account the movement of the target, and the expected position $\hat{x}^{(j)}$ of the target j can be predicted using the current estimates and the dynamic model of the target (Fig. 2(a)).

The generated path is discretized at specific intervals and used as waypoints for path tracking control to generate an initial guess of the control inputs. The path tracking problem can be formulated by defining a path as a sequence of desired waypoints $([p_x^{(i)}, p_y^{(i)}]_d^1, \dots, [p_x^{(i)}, p_y^{(i)}]_d^n, [p_x^{(i)}, p_y^{(i)}]_d^{n+1}, \dots)$. We construct a controller that reduces the angle between the line connecting the two adjacent waypoints and the heading direction of the UAV, and a damping effect is added to the controller for the stability. The geometry of the tracking problem is depicted in Fig. 2(b). The control input of the PD-controller can be computed with (4) as follows:

$$u_{t+1}^{(i)} = -K_p(\psi_t^{(i)} - \psi_d^{(i)}) - K_d\dot{\psi}_t^{(i)}, \quad (30)$$

where K_p and K_d are the gains of the controller.

B. Convergence and Complexity Analysis

The solution of ADMM for a nonconvex problem generally converges to a locally optimal point, and although its convergence is not guaranteed [27], ADMM has already been successfully applied in many applications [31]–[34]. In our application of ADMM, it is very important to set the appropriate penalty parameter ρ and to initialize the values in (18) and (19) properly. Too large values of ρ make the global common variable dominant in (18), and lead to less emphasis on reducing the uncertainty of the target. In order to select an appropriate value of ρ , extensions of the distributed ADMM algorithm have been explored. We would like to refer the readers to [27], [46]. In this work, the trajectory variables $[\mathbf{P}_j, \mathbf{U}_j]$ in (18) are initialized by the method described in Section III-A.2, and they are averaged to initialize the global common variables $[\mathbf{P}^C, \mathbf{U}^C]$.

The computational complexity of each iteration of the distributed ADMM is dominated by solving the subproblems defined in (18) because computing the global common variable and Lagrange multipliers requires very simple computations. The subproblems are solved by the belief space iLQG method described in Section III-A, and its computational complexity in the control problem is already

well analyzed in [40]. As with the control problem in [40], the bottleneck of running time in our problem lies in the calculation of the matrix $\mathbf{Q}_{vv,t}$ in (26). Let us define m and n as the state dimension of the target and the mobile sensors, respectively. As the belief state of the target contains the covariance matrix of the state, the dimension of the belief is $O[m^2]$. Accordingly, the dimension of the entire system is $O[m^2 + n]$, and computing the product $\mathcal{F}_{v,t}^\top \mathbf{V}_{vv,t+1} \mathcal{F}_{v,t}$ in (27) takes $O[(m^2 + n)^3]$ time. Evaluating $\ell_{vv,t}$ using numerical differentiation (central differences) can be done in $O[(m^2 + n)^3]$ time. The remaining elements do not form bottlenecks during computation, and detailed discussions can be found in [40]. One cycle of value iteration takes T steps, and thus its complexity is $O[T(m^2 + n)^3]$. The number of cycles cannot be expressed in terms of dimensional notation, but convergence can be expected after 10-100 cycles in practice. Furthermore, it is known that belief space iLQG converges with a second-order rate to a local optimum [40]. This work focuses on the problem of tracking multiple targets with a small number of UAVs, considering the area coverage capabilities of UAVs. Thus, we can assume that the total states dimension of UAVs is smaller than the belief state dimension of a target ($m^2 > n$). Then, one cycle of value iteration in the original problem (11) (not of the distributed optimization form) can be done in $O[TM^2m^6]$ time, assuming there is no correlation between the states of the target, where M is the number of targets to be tracked.

The computational complexity of our distributed trajectory optimization algorithm can be considered to replace M^2 in the original problem with the number of iterations of distributed ADMM if the computation is fully parallelized. ADMM is known to require a few tens of iterations to converge with modest accuracy for many applications [27], [34], [47]. Although our distributed framework can slightly increase the computational complexity of the problem when the number of targets to be tracked is small, this allows us to circumvent solving the task-assignment problem which is difficult even to configure. Many studies have been conducted to obtain solutions quickly for research on distributed optimization [31], [32], [46]. We present an edge-cutting method that effectively shortens the running time of our algorithm in the following section.

C. Edge-cutting Method

When a mobile sensor tracks multiple targets within a given planning time, it might be better to track some of them. Also, it may be more efficient for mobile sensors to track targets separately when multiple sensors track multiple targets. Empirically, these output characteristics can be obtained by the proposed algorithm. The proposed algorithm, however, continues to solve the trajectory optimization problem between a mobile sensor and a target whose uncertainty is not reduced by the mobile sensor during the iteration of the distributed optimization, which slows down the computation. To tackle this problem, we propose an edge-cutting method which cuts an edge and does not solve unnecessary problems (Fig. 3). The method evaluates each of the trajectories during the optimization process as follows:

$$\sum_{t=0}^T tr(Q\Sigma_t^{(j)}(\mathbf{p}_t^{-i})) - tr(Q\Sigma_t^{(j)}(\mathbf{p}_t)), \quad (31)$$

where $tr(Q\Sigma_t^{(j)}(\mathbf{p}_t^{-i}))$ denotes the uncertainty of target j under \mathbf{p}_t^{-i} is given, \mathbf{p}_t^{-i} denotes the states of the mobile sensors except mobile sensor i at time t . $tr(Q\Sigma_t^{(j)}(\mathbf{p}_t))$ is the amount of uncertainty about a target j when the states of all mobile sensors \mathbf{p}_t are given. If the evaluated value is less than the specified value ϵ , the corresponding edge is cut. Evaluating (31) requires an estimate of the target states. As in Section II-B, we apply the maximum-likelihood observations assumption to obtain an estimate of the target state in the absence of measurements. In addition, it is assumed that all trajectories except for the trajectory of the i -th mobile sensor use the trajectory obtained in the consensus phase given by (19). This method may sometimes generate a suboptimal solution, but it empirically appears to yield a result identical to the best solution in most situations. Problems that arise when using the edge-cutting method can be solved by a receding-horizon control scheme (Section III-D), and if ϵ is well adjusted, a reasonable result can be obtained. We note that the proposed method has the purpose of shortening the computation time of the problem, and if ϵ is not set to be too large, it provides the same result as the algorithm without the edge-cutting method.

Our edge-cutting method shares similarities with the message-passing algorithm in [31]. They apply the three-weight message-passing algorithm [32] for collision-free multi-agent trajectory planning, where one of two penalty weights ρ (zero and constant) is determined based on the results of each subproblem. Subproblems consist of minimizers that allow for finding trajectories with the minimal total energy, avoiding static obstacles, or imposing dynamic constraints. In our case, the subproblems are trajectory optimization problems that maximize the estimation performance for each target. Hence, they can be seen to play a role similar to that of the minimizers defined in [31] (the nodes on the left in Fig. 3(a)). However, in the informative trajectory planning problem, the measurements of the mobile sensors are correlated through the stochastic belief dynamics (9) of the targets (the nodes on the right in Fig. 3(a)). Thus, mobile

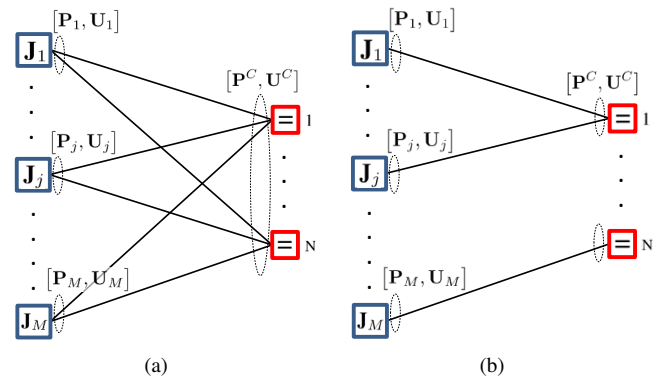


Fig. 3: (a) Fully connected bipartite graph, and (b) bipartite graph after applying the edge-cutting method

sensors cannot be separated without an approximation. The approximated problem is represented in the same form as the collision-free trajectory planning problem [31], which makes a solution to get stuck in bad local optima. If we apply aforementioned message-passing algorithm [31] to our informative trajectory planning problem, the penalty weight is set to 0 for the trajectory optimization result between a mobile sensor and a target whose uncertainty is not reduced by the mobile sensor, after which the equality-node of the corresponding edge is ignored in the consensus process. However, unnecessary mobile sensor-target pairs are consistently included in the trajectory optimization in each iteration of the ADMM, regardless of whether or not the penalty weight is set to zero. On the other hand, the proposed edge-cutting method separates the system integrated into the dynamics of mobile sensors through edge cutting to reduce the computation time more effectively. This method reduces the dimensions of the belief dynamics (9) during the optimization process. Specifically, applying the message-passing algorithm [31] to our problem maintains the graphs during the iteration of ADMM, but our method neglects the correlation between the measurements of the mobile sensors and transforms the graphs through cutting as shown in Fig. 3(b).

D. Receding Horizon Control

In a multi-target tracking problem, prior information about the targets is limited and the computation time for trajectory planning can become impractically long as the complexity of the problem increases. Thus, a receding-horizon control scheme (RHC) can be appropriate. RHC, also known as model predictive control (MPC), is a form of feedback (i.e., closed-loop) control system. With RHC, an optimization problem is solved at specific time intervals to determine a plan over a fixed time horizon and then the forepart of this plan is applied. The planning process is repeated by solving a new optimization problem, with the time horizon shifted a specific step forward. Optimization is performed based on available measurements and data at each step. Thus, the control policy involves feedback. The feedback

Algorithm 2 Receding-horizon control

```
1: Set control horizon  $T_c$  and planning horizon  $T_p$ 
2: Input  $\mathbf{p}_{init}$ ,  $\mathbf{b}_{init}$  and initial plan  $[\hat{\mathbf{P}}, \hat{\mathbf{U}}]$ 
3: while operation time is remaining do
4:   for  $t \leftarrow 1$  to  $T_c - 1$  do
5:     if  $t = 1$  then
6:        $\hat{\mathbf{b}} = \text{GAUSSIAN APPROXIMATION}(\mathbf{b}_{t+1})$ 
7:        $\hat{\mathbf{b}}_{T_c} = \text{PROPAGATE}(\hat{\mathbf{b}}, T_c)$ 
8:        $[\hat{\mathbf{P}}, \hat{\mathbf{U}}]_{new}$ 
         =  $\text{CREATE PLAN}(\hat{\mathbf{b}}_{T_c}, [\hat{\mathbf{P}}_{T_c}, \hat{\mathbf{U}}_{T_c}], T_p)$ 
          $\triangleright$  Algorithm 1.
9:     end if
10:     $\mathbf{b}_{t+1} = \text{EXECUTE PLAN}([\hat{\mathbf{P}}, \hat{\mathbf{U}}], t)$ 
11:  end for
12:   $[\hat{\mathbf{P}}, \hat{\mathbf{U}}] = [\hat{\mathbf{P}}, \hat{\mathbf{U}}]_{new}$ 
13: end while
```

control scheme enables real-time measurements to be used to determine the control input, and it can compensate for a deviation between the predicted and actual output that can be caused by system-model mismatches and disturbances.

Our RHC strategy is shown in Algorithm 2. In situations where a non-linear tracking filter is utilized for the estimation of the target information, we approximate a target distribution into a Gaussian distribution for planning purposes (line 6). One important point during the real-time implementation of the algorithm is that the future plan should be pre-calculated, which requires future information of targets. To predict the future information of targets, we use the maximum likelihood assumption and estimate the target information with no measurements (line 7). A new plan $[\hat{\mathbf{P}}, \hat{\mathbf{U}}]_{new}$ for the future time step T_p is created using the proposed distributed trajectory optimization algorithm (line 8). Here, we use the estimated future information of targets under the maximum likelihood assumption simultaneously with the previous plan at the control horizon T_c . The planning horizon, T_p , should be large enough so that the trajectories of the mobile sensors can cover the overall domain of interest. Solving this problem provides the input commands of the mobile sensors for the T_p future time steps. However, only a forepart of these T_p input commands is actually implemented (line 8). We denote this subset as control horizon T_c , which is determined by the available computational resources and the communication delay ($T_c \leq T_p$). The process is then repeated, and a new set of commands is developed for the next time window.

IV. SIMULATIONS

In this section, we numerically investigate the computational properties and the applicability of the proposed algorithms. We assume that UAVs fly at different altitudes from each other to alleviate collision-avoidance constraints. In all of our tests, the planning horizon, T_p , is set to 100 seconds, which is the time required to cover all areas of interest when UAVs are flying at a speed of $16m/s$. A target motion is assumed by (2), with the time interval between

two successive measurements $dt = 0.1s$ and the constant diffusion strength $q = 0.01$. The sensors are mounted on the left or right sides of the UAVs and are aimed in a 30-degree downward direction. The parameters of the measurement model (6) are $\alpha = 10$, $\gamma = 8\ln 2$ and $\beta = 0$. In (18), we chose $Q = I$ and $R = 100$. Furthermore, we selected $\rho_v = [0.02, 0.02, 500 \times 180/\pi, 500 \times 180/\pi]^T$, $\rho_u = 500 \times 180/\pi$, $\alpha_v = 0.2\rho_v$ and $\alpha_u = 0.2\rho_u$ in (20).

To ascertain the effectiveness of the distributed trajectory optimization algorithm, we compared the algorithm with existing approaches; myopic trajectory planning [5], [18], non-myopic trajectory planning [3], and two-phase approaches [5], [18], [23]. The myopic trajectory planning method performs one-step trajectory optimization [5], [18]. Therefore, we repeatedly performed one-step trajectory optimization during the planning horizon for a fair comparison of the myopic and non-myopic trajectory planning methods. The initial guess generation method that can be easily adopted in the multi-step local trajectory optimization is to input zero control commands to the dynamics and generate an initial guess trajectory [3]. Two-phase approaches [5], [18], [23] cluster the targets and assign the clusters to the mobile sensors. Then, myopic trajectory optimization is performed based on the task-assignment results. For a fair comparison of our algorithm with the two-phase approaches, we use only clustering and task-assignment algorithms of the two-phase approaches and combine them with the non-myopic trajectory planning method described in (11) and Section III-A. Initial guesses are generated so that the UAV can visit the clusters sequentially based on the task-assignment results in a manner similar to that described in Section III-A.2; these are shown as the dotted lines in Figs. 5(c-d). In [18], the priority of each cluster is defined as the sum of the uncertainties of the targets included in the cluster at $t = 0$ (i.e., the planning time). The cluster with a higher priority is then assigned to the mobile sensor that is closest to the center of the cluster sequentially. In [23], the number of targets in each cluster and the Euclidean distance between the center of the mobile sensor and clusters are used to prioritize clusters.

For the first example, we considered a simple scenario consisting of a single UAV and two stationary targets to show the process of converging on a solution through the distributed trajectory optimization algorithm. Fig. 4(a) shows the resulting trajectory when one-step myopic trajectory planning is repeated. The sensor has a limited field of view, and all targets are located out of view at the planning time and one-time step later. Thus, the current control effort is not propagated in the future time step, and an optimal solution is obtained that minimizes the control effort only [21], [25]. The proposed algorithm, on the other hand, provides a non-myopic trajectory planning result that sequentially tracks two targets, as shown in Fig. 4(b). Figs. 4 (d-g) present snapshots of the optimization process and the results. The consensus trajectory is obtained through the optimization results of each subproblem, which affects the optimization in the next iteration through the Lagrange multipliers; that is, the optimization results of each subproblem reflect the op-

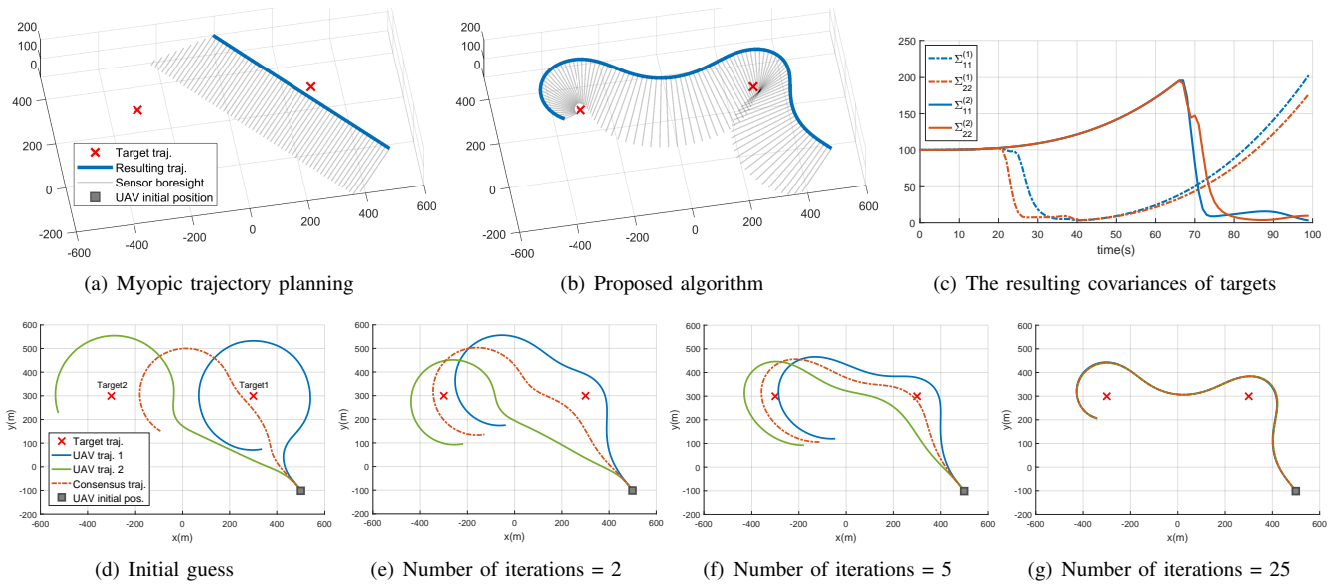


Fig. 4: (a)-(b) Comparison of myopic planning [5], [18] and the proposed non-myopic planning in a scenario with a single UAV and two stationary targets, (c) the resulting covariances of targets, and (d)-(g) process of converging on a solution

timization process of the other subproblems of the previous iteration. This procedure is repeated, and finally we obtain the converged solution.

In the second example, we compared the proposed algorithm with existing approaches for three cases where the number of targets to be tracked is different, with one UAV. The targets are assumed to be stationary, and the initial positions in the x - y space of the UAV and the targets are randomly generated within $1200m \times 1200m$ areas. The targets are on the ground and the UAVs are flying at a fixed altitude of $100m$. The initial uncertainty of the targets is randomly generated between 10 and 100 of the diagonal component of the covariance matrix, and the remaining components are set to zero. In this example, the number of targets to be tracked is not large; therefore, clustering for assigning tasks in the two-phase approaches is excluded. We note that even if clustering algorithms are used, the order in which the targets within each cluster should be tracked should be determined. Fig. 5 shows one instance in scenarios with three targets. UAVs can visit anywhere in the area within the set planning horizon time, but it can be difficult to visit multiple locations. Making the planning horizon time longer can greatly increase the computation time of the algorithm. Accordingly, intelligent decision-making is required, but it may not be easy in general. The results clearly shows the impact of the decision-making (i.e., the initial guess) on the solution. The myopic trajectory planning algorithm minimizes control efforts only before the target enters the field of view of the sensor as shown in the Fig. 5(a), as the current control effort is not propagated to future time steps. That is, current control efforts do not help to improve future estimation performance outcomes. Fig. 5(b) shows that performing non-myopic trajectory optimization without proper decision making could get stuck in bad

local optima. The two-phase approaches can also provide a local optimal solution because they use approximate/heuristic cost functions for task-assignment without considering the mobility of the sensor platform and changes in the target state over time (Figs. 5(c-d)). On the other hand, the proposed algorithm results different from those of the previous methods as shown in Fig. 5(e). Our algorithm does not require the definition of a new cost function for task assignment, as it incorporates decision making into the optimization process while considering the mobility of the sensor platform and the target state through the distributed formulation. Because both targets on the left and right cannot be tracked at the same time, the trajectory is optimized to track the target on the right with greater uncertainty than the target on the left and then the target with the greatest uncertainty is tracked. Although the proposed algorithm does not guarantee global optimality, it achieves better performance on average than the other methods, as shown in Table I.

The third example considers the situation in which two UAVs track multiple targets. The simulation settings are identical except for the two UAVs. For the execution of our algorithm, the initial guesses for each of the pairs of targets and UAVs are generated in the same manner used in the previous examples. The algorithm is compared with the two-phase approaches [18], [23] involving target clustering. Density-based spatial clustering of applications with noise (DBSCAN) [24] is used as the clustering algorithm. In order to initiate clustering, DBSCAN requires two parameters: the minimum number of points needed to form a cluster and the maximum distance around a point. These were set to 2 and $150m$, respectively. Fig. 6 shows the resulting trajectories of the proposed algorithm and the two-phase approaches in one of the ten targets tracking scenarios. Euclidean heuristic and uncertainty-based task assignments give the same result

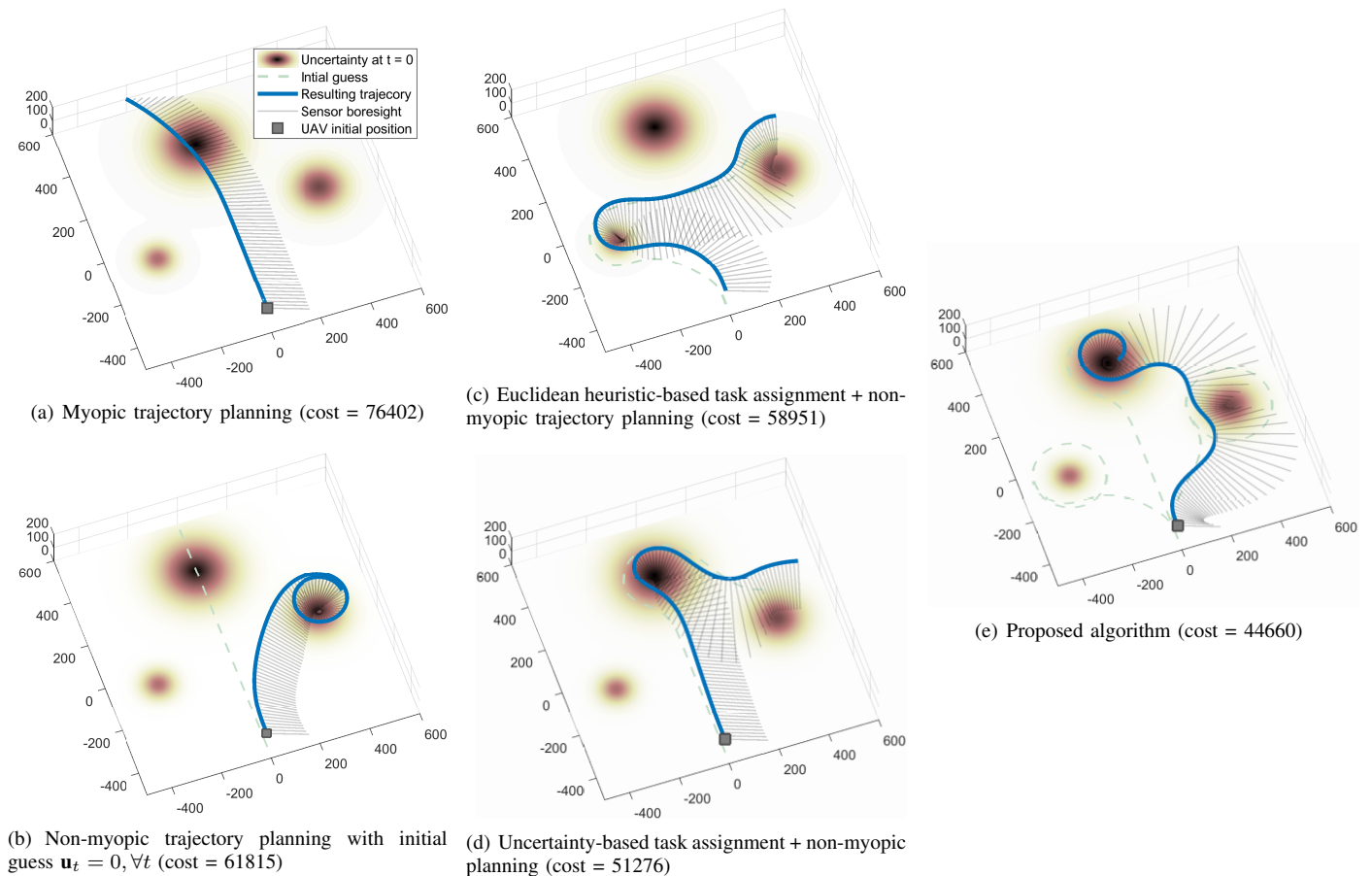


Fig. 5: Comparison of existing approaches and the proposed algorithm in a scenario with a single UAV and three stationary targets

TABLE I: Average costs from 100 simulations with each algorithm in the single UAV scenario.

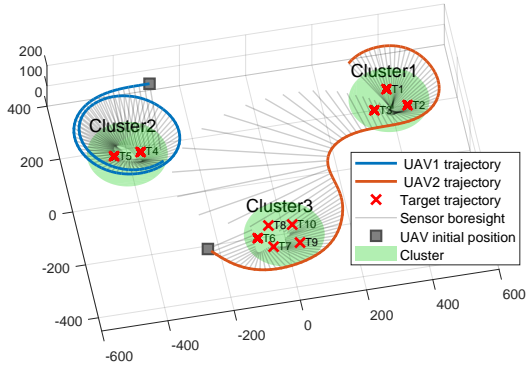
Number of targets	2	3	4
Myopic trajectory planning [5], [18]	63577	79521	128627
Non-myopic trajectory planning with initial guess $\mathbf{u}_t = 0, \forall t$ [3]	52361	63624	94937
Euclidean heuristic-based task assignment [23] + non-myopic trajectory planning	34731	54432	73761
Uncertainty-based task assignment [18] + non-myopic trajectory planning	33862	52319	70246
Proposed distributed trajectory optimization algorithm	25153	45680	60241

TABLE II: Average costs from 100 simulations with each algorithm for a scenario with two UAVs.

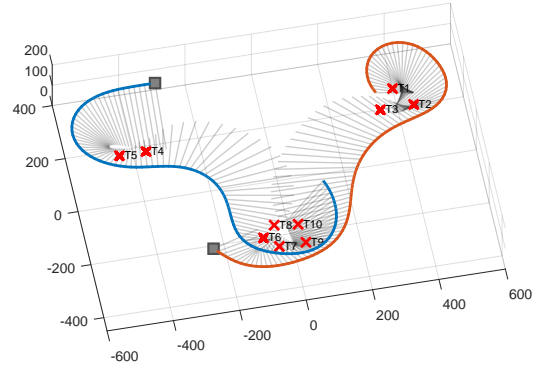
Number of targets	10	15
Target clustering & Euclidean heuristic-based task assignment [23] + non-myopic trajectory planning	562576	755267
Target clustering & uncertainty-based task assignment [18] + non-myopic trajectory planning	572217	760146
Proposed distributed trajectory optimization algorithm	393481	571241

in the scenario, where each cluster is assigned to only one UAV. The proposed algorithm automatically generates trajectories optimized for mobile sensors to visit the target clusters without the aid of clustering and task-assignment algorithms. Furthermore, the proposed algorithm provides trajectories for two UAVs to visit the same cluster, which is not allowed in the case of two-phase approaches. Table II shows that the proposed algorithm outperforms the two-phase approaches on average in randomly generated scenarios. Figs. 7(a-c) show that the edges are maintained and cut for different ϵ values. If the set ϵ value is not large, the

same result can be obtained as in cases where the edge-cutting method is not applied ($\epsilon = 0$), as shown in Fig. 7(d) and Fig. 6(b). Specifically, when the epsilon value is set appropriately, trajectory optimization associated with the cut edges is excluded, reducing the dimensions of the subproblems. The computation time comparison is performed on a 3.40 GHz Intel(TM) i7 PC that can use six computational devices. As shown in Figs. 7(d-f), parallel computing reduces the computation time, and if the ϵ value is properly set, the edge-cutting method can reduce the computation time while achieving the same result. The use of the message-

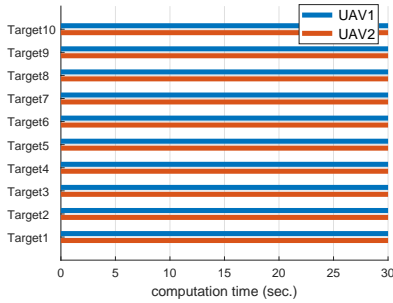


(a) Target clustering & Euclidean heuristic/uncertainty-based task assignment + non-myopic trajectory planning (cost = 590571)

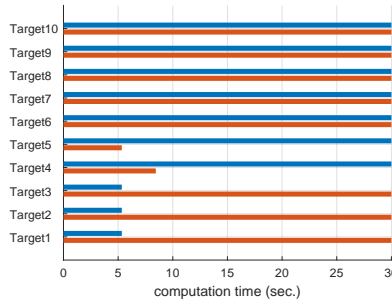


(b) Proposed algorithm (cost = 352713)

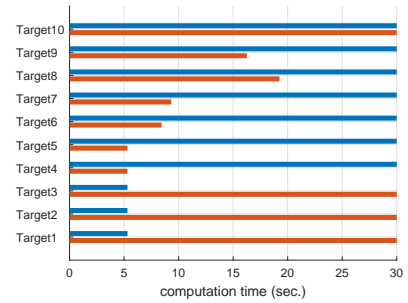
Fig. 6: Comparison of two-phase approaches and the proposed algorithm for a scenario with two UAVs and ten stationary targets



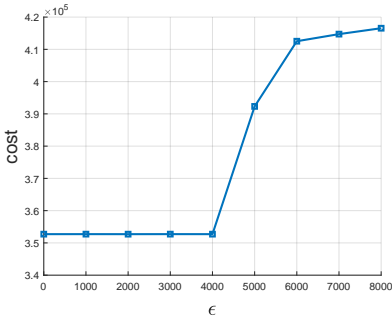
(a) $\epsilon = 0$, Two-weights message passing



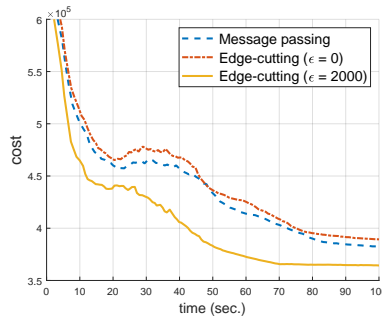
(b) $\epsilon = 2000$



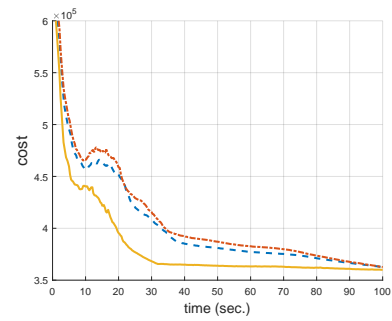
(c) $\epsilon = 6000$



(d) Cost comparison w.r.t. ϵ value



(e) Results without parallel computing



(f) Results with parallel computing

Fig. 7: (a)-(c) Result of the application of the edge-cutting method according to the ϵ value (the lines indicate that the corresponding targets are considered in the trajectory optimization process of the UAVs), (d) cost comparison w.r.t. the ϵ value, and (e)-(f) comparison of the computation times

passing algorithm in [31] for our problem may reduce the computation time slightly, but the effect is less than that of the proposed edge-cutting method.

In the last example, shown in Fig. 8, we considered two UAVs, one target moving at a speed of 3m/s in the x-axis direction, and two stationary targets. We applied the distributed trajectory optimization algorithm, the edge-cutting method, and RHC scheme together. It is assumed that a particle filter is used to estimate the states of the target in the actual operating environment of the UAVs. The control

horizon, T_c , is set to 25 seconds considering the computation time of the algorithms. It is assumed that the sensors are attached to the left side of one UAV and to the right side of the other UAV, and that UAVs fly at different altitudes of 100m and 120m, respectively. Figs. 8(a-d) show some of the simulated results under the assumption that the UAVs operate for 400 seconds. A notable point in this example is that the UAV automatically passes the tracking mission to the other UAV after about 160 seconds. Figs. 8(e-f) show the state estimation results of the targets, where it can be confirmed

that all targets are tracked reliably through the RHC scheme.

V. CONCLUSIONS

In this paper, we investigated a distributed optimization approach to trajectory planning for a multi-target tracking problem. In order to solve the trajectory optimization and task-assignment problems simultaneously, the distributed trajectory optimization problem was formulated, and then solved by integrating a variant of a differential dynamic programming algorithm called iterative Linear-Quadratic-Gaussian (iLQG) algorithm with the distributed Alternating Direction Method of Multipliers (ADMM) method. In addition, we proposed an edge-cutting method to reduce the computation time of the algorithm and the RHC scheme for real-time implementation. Numerical experiments were conducted and the results presented to demonstrate the applicability and validity of the proposed approach.

REFERENCES

- [1] M. Dunbabin and L. Marques, "Robots for environmental monitoring: Significant advancements and applications," *IEEE Robotics & Automation Magazine*, vol. 19, no. 1, pp. 24–39, 2012.
- [2] Q. Yang and S.-J. Yoo, "Optimal uav path planning: Sensing data acquisition over iot sensor networks using multi-objective bio-inspired algorithms," *IEEE Access*, vol. 6, pp. 13 671–13 684, 2018.
- [3] S. S. Ponda, R. M. Kolacinski, and E. Frazzoli, "Trajectory optimization for target localization using small unmanned aerial vehicles," Ph.D. dissertation, Massachusetts Institute of Technology, Department of Aeronautics and Astronautics, 2008.
- [4] Y. Oshman and P. Davidson, "Optimization of observer trajectories for bearings-only target localization," *IEEE Transactions on Aerospace and Electronic Systems*, vol. 35, no. 3, pp. 892–902, 1999.
- [5] H. Oh, S. Kim, H.-s. Shin, and A. Tsourdos, "Coordinated standoff tracking of moving target groups using multiple uavs," *IEEE Transactions on Aerospace and Electronic Systems*, vol. 51, no. 2, pp. 1501–1514, 2015.
- [6] G. M. Hoffmann and C. J. Tomlin, "Mobile sensor network control using mutual information methods and particle filters," *IEEE Transactions on Automatic Control*, vol. 55, no. 1, pp. 32–47, 2010.
- [7] H.-L. Choi and S.-J. Lee, "A potential-game approach for information-maximizing cooperative planning of sensor networks," *IEEE Transactions on Control Systems Technology*, vol. 23, no. 6, pp. 2326–2335, 2015.
- [8] S. Ragi and E. K. Chong, "Uav path planning in a dynamic environment via partially observable markov decision process," *IEEE Transactions on Aerospace and Electronic Systems*, vol. 49, no. 4, pp. 2397–2412, 2013.
- [9] S. A. Miller, Z. A. Harris, and E. K. Chong, "A pomdp framework for coordinated guidance of autonomous uavs for multitarget tracking," *EURASIP Journal on Advances in Signal Processing*, vol. 2009, p. 2, 2009.
- [10] H.-L. Choi, J. P. How, and P. I. Barton, "An outer-approximation approach for information-maximizing sensor selection," *Optimization Letters*, vol. 7, no. 4, pp. 745–764, 2013.
- [11] C. Taylor, A. Rahimi, J. Bachrach, H. Shrobe, and A. Grue, "Simultaneous localization, calibration, and tracking in an ad hoc sensor network," in *Proceedings of the 5th international conference on Information processing in sensor networks*. ACM, 2006, pp. 27–33.
- [12] Y. Bar-Shalom, X. R. Li, and T. Kirubarajan, *Estimation with applications to tracking and navigation: theory algorithms and software*. John Wiley & Sons, 2004.
- [13] J. L. Williams, J. W. Fisher, and A. S. Willsky, "Approximate dynamic programming for communication-constrained sensor network management," *IEEE Transactions on signal Processing*, vol. 55, no. 8, pp. 4300–4311, 2007.
- [14] C. Kreucher, A. O. Hero, K. Kastella, and D. Chang, "Efficient methods of non-myopic sensor management for multitarget tracking," in *Decision and Control, 2004. CDC. 43rd IEEE Conference on*, vol. 1. IEEE, 2004, pp. 722–727.
- [15] A. S. Chhetri, D. Morrell, and A. Papandreou-Suppappola, "Energy efficient target tracking in a sensor network using non-myopic sensor scheduling," in *Information Fusion, 2005 8th International Conference on*, vol. 1. IEEE, 2005, pp. 8–pp.
- [16] S.-J. Lee, Y.-J. Park, and H.-L. Choi, "Efficient sensor network planning based on approximate potential game," *International Journal of Distributed Sensor Networks*, vol. 14, no. 6, pp. 1–17, 2018.
- [17] A. S. Chhetri, D. Morrell, and A. Papandreou-Suppappola, "Nonmyopic sensor scheduling and its efficient implementation for target tracking applications," *EURASIP Journal on Applied Signal Processing*, vol. 2006, pp. 9–9, 2006.
- [18] N. Farmani, L. Sun, and D. J. Pack, "A scalable multitarget tracking system for cooperative unmanned aerial vehicles," *IEEE Transactions on Aerospace and Electronic Systems*, vol. 53, no. 4, pp. 1947–1961, 2017.
- [19] P. Skoglar, *UAV path and sensor planning methods for multiple ground target search and tracking-A literature survey*. Linköping University Electronic Press, 2007.
- [20] H. Jiang and Y. Liang, "Online path planning of autonomous uavs for bearing-only standoff multi-target following in threat environment," *IEEE Access*, vol. 6, pp. 22 531–22 544, 2018.
- [21] S.-J. Lee, S.-S. Park, and H.-L. Choi, "Potential game-based non-myopic sensor network planning for multi-target tracking," *IEEE Access*, vol. 6, pp. 79 245–79 257, 2018.
- [22] F. Cheng, S. Zhang, Z. Li, Y. Chen, N. Zhao, F. R. Yu, and V. C. Leung, "Uav trajectory optimization for data offloading at the edge of multiple cells," *IEEE Transactions on Vehicular Technology*, vol. 67, no. 7, pp. 6732–6736, 2018.
- [23] B. Luders, D. Levine, S. Ponda, and J. How, "Information-rich task allocation and motion planning for heterogeneous sensor platforms," in *Infotech@ Aerospace 2011*, 2011, p. 1588.
- [24] M. Ester, H.-P. Kriegel, J. Sander, X. Xu *et al.*, "A density-based algorithm for discovering clusters in large spatial databases with noise," in *Kdd*, vol. 96, no. 34, 1996, pp. 226–231.
- [25] J. Liu, D. Petrovic, and F. Zhao, "Multi-step information-directed sensor querying in distributed sensor networks," in *2003 IEEE International Conference on Acoustics, Speech, and Signal Processing, 2003. Proceedings.(ICASSP'03)*, vol. 5. IEEE, 2003, pp. V–145.
- [26] D. Levine, B. Luders, and J. P. How, "Information-rich path planning with general constraints using rapidly-exploring random trees," 2010.
- [27] S. Boyd, N. Parikh, E. Chu, B. Peleato, J. Eckstein *et al.*, "Distributed optimization and statistical learning via the alternating direction method of multipliers," *Foundations and Trends® in Machine Learning*, vol. 3, no. 1, pp. 1–122, 2011.
- [28] J. F. Mota, J. M. Xavier, P. M. Aguiar, and M. Püschel, "D-admm: A communication-efficient distributed algorithm for separable optimization," *IEEE Transactions on Signal Processing*, vol. 61, no. 10, pp. 2718–2723, 2013.
- [29] R. Zhang and J. Kwok, "Asynchronous distributed admm for consensus optimization," in *International Conference on Machine Learning*, 2014, pp. 1701–1709.
- [30] H. Y. Ong and J. C. Gerdes, "Cooperative collision avoidance via proximal message passing," in *2015 American Control Conference (ACC)*. IEEE, 2015, pp. 4124–4130.
- [31] J. Bento, N. Derbinsky, J. Alonso-Mora, and J. S. Yedidia, "A message-passing algorithm for multi-agent trajectory planning," in *Advances in neural information processing systems*, 2013, pp. 521–529.
- [32] N. Derbinsky, J. Bento, V. Elser, and J. S. Yedidia, "An improved three-weight message-passing algorithm," *arXiv preprint arXiv:1305.1961*, 2013.
- [33] I. Mordatch and E. Todorov, "Combining the benefits of function approximation and trajectory optimization," in *Robotics: Science and Systems*, 2014.
- [34] S. Liu, M. Fardad, E. Masazade, and P. K. Varshney, "Optimal periodic sensor scheduling in networks of dynamical systems," *IEEE Transactions on Signal Processing*, vol. 62, no. 12, pp. 3055–3068, 2014.
- [35] Y. Bar-Shalom, P. K. Willett, and X. Tian, *Tracking and data fusion*. YBS publishing, 2011.
- [36] A. B. Charlish, "Autonomous agents for multi-function radar resource management," Ph.D. dissertation, UCL (University College London), 2011.
- [37] M. I. Skolnik, "Radar handbook," 1970.
- [38] H.-L. Choi and J. P. How, "On the roles of smoothing in planning of

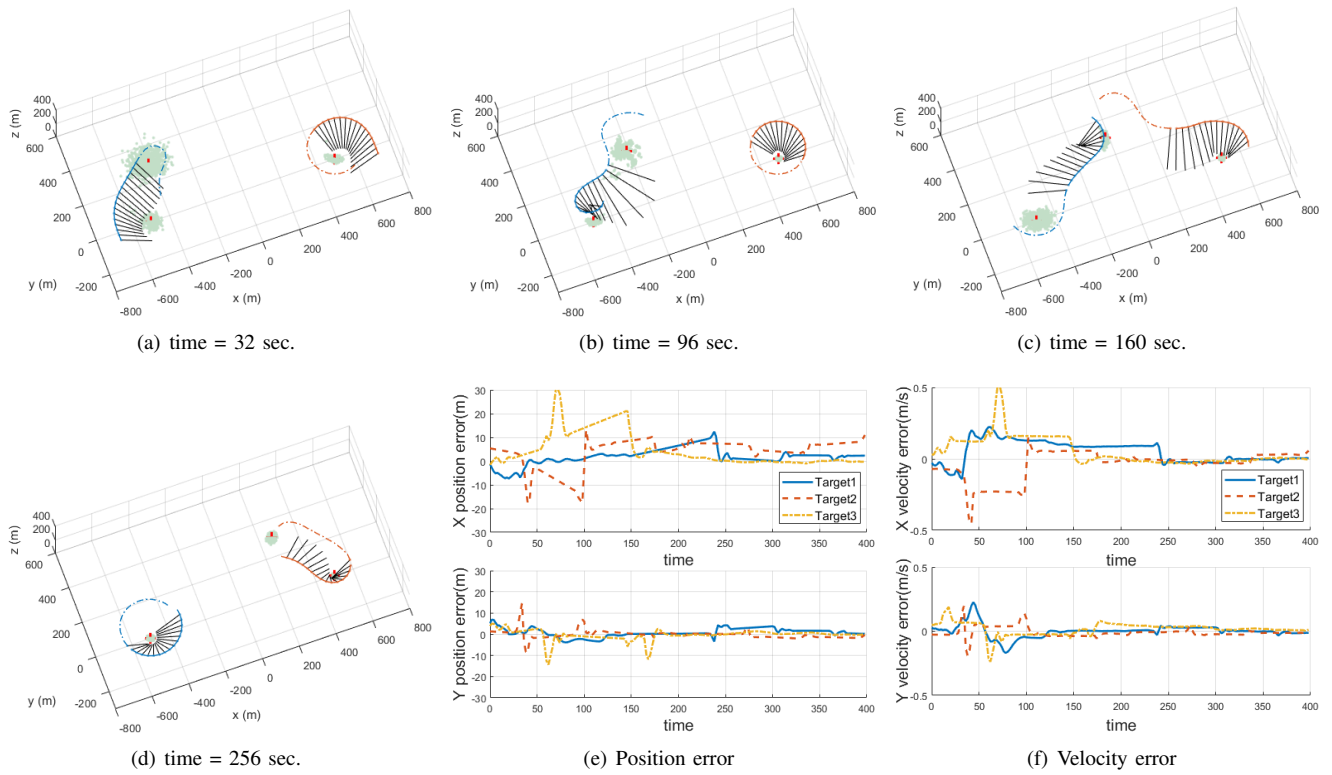


Fig. 8: (a)-(d) Snapshots of the current plan (solid line) and future plan (dashed line) for each mobile sensor in the replanning process scenario with two UAVs, one moving target and two stationary targets, and (e)-(f) particle filter estimation results

- informative paths,” in *American Control Conference, 2009. ACC’09*. IEEE, 2009, pp. 2154–2159.
- [39] Z. Chen *et al.*, “Bayesian filtering: From kalman filters to particle filters, and beyond,” *Statistics*, vol. 182, no. 1, pp. 1–69, 2003.
- [40] J. Van Den Berg, S. Patil, and R. Alterovitz, “Motion planning under uncertainty using iterative local optimization in belief space,” *The International Journal of Robotics Research*, vol. 31, no. 11, pp. 1263–1278, 2012.
- [41] R. Platt Jr, R. Tedrake, L. Kaelbling, and T. Lozano-Perez, “Belief space planning assuming maximum likelihood observations,” 2010.
- [42] E. Wei and A. Ozdaglar, “Distributed alternating direction method of multipliers,” 2012.
- [43] E. Todorov and W. Li, “A generalized iterative lqg method for locally-optimal feedback control of constrained nonlinear stochastic systems,” in *American Control Conference, 2005. Proceedings of the 2005*. IEEE, 2005, pp. 300–306.
- [44] D. H. Jacobson and D. Q. Mayne, “Differential dynamic programming,” 1970.
- [45] L. E. Dubins, “On curves of minimal length with a constraint on average curvature, and with prescribed initial and terminal positions and tangents,” *American Journal of mathematics*, vol. 79, no. 3, pp. 497–516, 1957.
- [46] C. Song, S. Yoon, and V. Pavlovic, “Fast admm algorithm for distributed optimization with adaptive penalty,” in *AAAI*, 2016, pp. 753–759.
- [47] E. Masazade, M. Fardad, and P. K. Varshney, “Sparsity-promoting extended kalman filtering for target tracking in wireless sensor networks,” *IEEE Signal Processing Letters*, vol. 19, no. 12, pp. 845–848, 2012.